

Development of an Enantioselective [3 + 2] Cycloaddition To Synthesize the Pyrrolidine Core of ABBV-3221 on Multikilogram Scale

John Hartung,^{*,†} Stephen N. Greszler,[‡] Russell C. Klix,[†] and Jeffrey M. Kallemeyn[†]

[†]Process Research and Development, AbbVie, Inc., 1 North Waukegan Road, North Chicago, Illinois 60064, United States

[‡]Discovery Chemistry and Technology, AbbVie, Inc., 1 North Waukegan Road, North Chicago, Illinois 60064, United States

Supporting Information

ABSTRACT: The tetrasubstituted pyrrolidine core of ABBV-3221 was synthesized by catalytic, enantioselective cycloaddition. A Cu(I) catalyst system was identified as ideal for further development, which gave a 78% yield of 99% purity product after optimization. The processes of catalyst selection, optimization, and crystallization of the cycloaddition product are described herein.

KEYWORDS: enantioselective catalysis, copper, [3 + 2] cycloaddition, pyrrolidine

INTRODUCTION

Cystic fibrosis (CF) is a debilitating and ultimately fatal genetic disease impacting more than 70 000 people worldwide.¹ CF is caused by a large variety of mutations leading to dysfunction of the cystic fibrosis transmembrane receptor (CFTR) protein,² which is responsible for anion transport in tissues throughout the body.³ Malfunction of the CFTR protein results in recurring lung infections and pancreatic insufficiency due to buildup of mucus. ABBV-3221 is a modulator of the CFTR protein in development as a potential therapy for cystic fibrosis.⁴ (See Figure 1.)

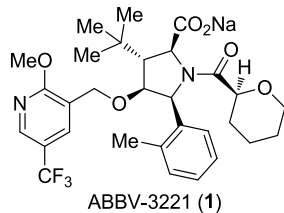


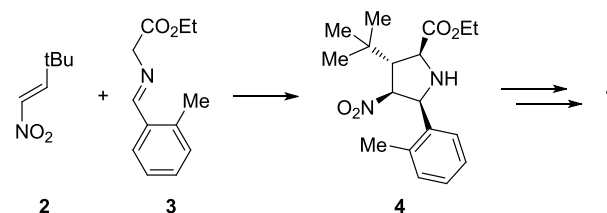
Figure 1. Structure of ABBV-3221.

The structure of **1** is dominated by its penta-substituted pyrrolidine core containing four contiguous stereocenters. Given the challenges in rejecting stereoisomeric impurities, a highly stereoselective transformation was required to limit the formation of the 15 undesired stereoisomers arising from the four stereocenters. The stereogenic tetrahydropyranyl amide, epimerizable carboxylate functionality, and sterically bulky *tert*-butyl group appended on the pyrrolidine core further contributed to the candidate's structural complexity. A strategy to synthesize **1** would require a robust transformation to set the ring stereochemistry while accommodating significant

steric interactions from the *tert*-butyl group and enabling further elaboration with the ether and amide substituents.

Early in our efforts it was established that an enantioselective [3 + 2] cycloaddition was an ideal method to forge the stereogenic pyrrolidine core in a convergent manner using a mature synthetic methodology.^{5–8} To achieve acceptable reactivity in the cycloaddition, an activating nitro group was appended on the olefin component that could later be converted to the requisite ether linkage by functional group interconversion.^{8,9} (See Scheme 1.)

Scheme 1. Abbreviated Synthetic Strategy toward ABBV-3221

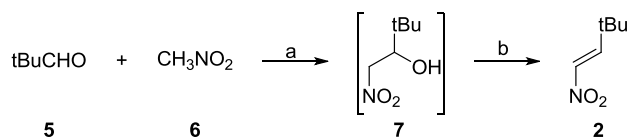


In the project's transition from Discovery to Process chemistry, work was carried out to develop a robust and scalable cycloaddition to fuel multikilogram synthesis of ABBV-3221. In particular, identification of a catalyst system, optimization of reaction parameters impacting stereoselectivity, and controls for process-related impurities impacting catalytic activity were explored to achieve an optimized process. Ultimately, a streamlined process utilizing crude imine in the enantioselective [3 + 2] cycloaddition and subsequent crystallization of high-purity pyrrolidine product directly from the reaction mixture was successfully executed on a multikilogram scale.

RESULTS AND DISCUSSION

Synthesis of Cycloaddition Starting Materials. Nitro olefin **2** was synthesized by condensation of nitromethane and pivaldehyde, and subsequent elimination mediated by trifluoroacetic anhydride (TFAA) and triethylamine (Scheme 2).¹⁰ The condensation produced varying amounts of **7** and **2**, which were funneled to **2** upon treatment with TFAA and

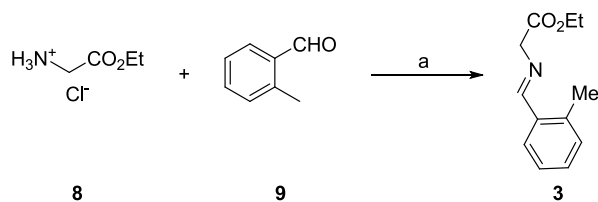
Received: June 27, 2019

Scheme 2. Synthesis of Nitro Olefin 2^a

^aReagents and conditions: (a) 5 (1.0 equiv), 6 (1.1 equiv), sodium hydroxide (1.3 equiv), ethanol, 0–10 °C, 1 h; (b) TFAA (1.15 equiv), triethylamine (2.3 equiv), methylene chloride, –15 to –10 °C, 1 h, 65% yield.

triethylamine. Product 2 was purified by column chromatography to give an isolated yield of 65% at 99% purity.

Imine 3 was synthesized by condensation of glycine ethyl ester hydrochloride with *ortho*-tolualdehyde in the presence of triethylamine and drying agent in methylene chloride (Scheme 3).¹¹ Higher yields were obtained by sequestration of water

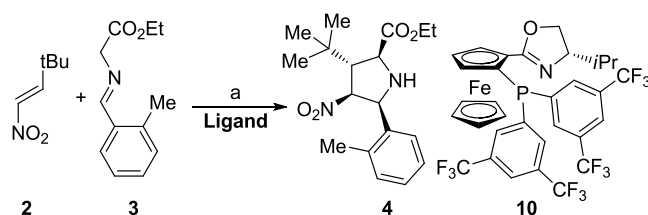
Scheme 3. Synthesis of Imine Reactant 3^a

^aReagents and Conditions: (a) 8 (1.1 equiv), 9 (1.0 equiv), triethylamine (1.1 equiv), sodium sulfate (anhydrous, 2.0 equiv), methylene chloride, 20 °C, 2 h, 93% yield.

with drying agent (magnesium or sodium sulfate) than with azeotropic distillation (Dean–Stark apparatus). Azeotropic removal of water resulted in decomposition of the imine due to its thermal instability.¹² Residual solids after workup could be minimized by using sodium sulfate over magnesium sulfate.

Rejection of reaction byproduct triethylamine HCl, excess 8, and drying agent could be achieved by filtration and washing of the organic layer with water and brine. The resultant solution of 3 in methylene chloride was solvent swapped to cyclopentyl methyl ether (CPME; to a final concentration of 45% w/w) to give a potency adjusted yield of 93%. The CPME solution was then used directly in the cycloaddition reaction. The two starting materials are the only impurities observed in isolated 3 in this process (8 0.7% w/w, 9 0.5% w/w), which did not have an impact on downstream chemistry. The resulting solution of 3 in CPME (45% w/w) was stable for up to 7 days at 0 °C as determined by qNMR.

Cu-Catalyzed Enantioselective Cycloaddition. Development of the [3 + 2] cycloaddition reaction was focused on achieving high reaction stereoselectivity, yield, and reproducibility at what was deemed an acceptable catalyst loading of approximately 1 mol %. Discovery efforts toward related pyrrolidines were aided by an enantioselective and high-yielding [3 + 2] cycloaddition catalyzed by Cu(I) and ligand 10.¹³ A high-throughput screen of Cu(I)/ligand complexes was carried out to exclude potentially more efficient or lower-cost alternatives to the initially identified system (Scheme 4 and Table 1; see the SI for full details). An array of ligands was combined with the precatalyst [Cu(OTf)₂]*toluene and catalytic base¹⁴ to form the requisite azomethine ylide from imine 3. A high *endo* diastereomeric ratio (dr) was observed with diverse ligand scaffolds and electronics. Ligands achieving >80% ee

Scheme 4. Design of Catalyst Screen for Cu-Catalyzed Enantioselective [3 + 2] Cycloaddition^a

^aReagents and conditions: (a) 2 (2 μmol, 1.0 equiv), 3 (2.2 μmol, 1.1 equiv), [Cu(OTf)₂]*toluene (0.1 μmol, 5 mol %), ligand (0.22 or 0.44 μmol, 10 or 20 mol %), KOtBu (0.16 μmol, 8 mol %), THF, 0 °C, 18 h.

Table 1. Selected Results from Catalyst Screen

Ligand	Conversion (%)	d.r. <i>endo/exo</i>	e.r. <i>endo</i>
	100	83:17	99.5:0.5
	100	95:5	94:6
	100	97:3	90:10
	77	61:39	91:9
	98	42:58	91:9

were limited to Segphos and push–pull bidentate ferrocenyl derivatives, with 10 affording significantly higher enantioselectivity compared to ferrocenyl bisphosphines (Table 1). The results of the screen clearly indicated that ligand 10 gave the highest enantioselectivity (99.5:0.5 er *endo* product; er, enantiomeric ratio), complete conversion, and acceptable diastereoselectivity (83:17 dr *endo/exo*) and was the lead for further development.^{8a}

The impact of reaction parameters on reaction outcome with CuOTf/10 were investigated to reduce catalyst loading from the initial screening level of 10 mol % and further optimize stereoselectivity and yield. Studies aimed at reducing catalyst loading determined that 0.25 mol % [Cu(OTf)₂]*C₆H₆ and 0.55 mol % 10 were minimally required

for full conversion (Table 2). Below this quantity, conversion and reaction er dropped significantly, and dr of the product

Table 2. Optimization of Precatalyst, Ligand, and Base Charge^a

[Cu(OTf) ₂ ·C ₆ H ₆ mol %]	10 mol %	KOtBu mol %	yield	dr	er <i>endo</i>
0.5	1.1	0.8	92	7:1	98.5:1.5
0.25	0.55	0.4	87	8.6:1	98.2:1.8
0.125	0.275	0.2	18 ^b	13:1	70:30

^aConditions: **2** (1.0 equiv), **3** (1.1 equiv), CPME (1 M in **3**), 0 °C, 0.5 h. ^bYield after 1.5 h.

increased, indicative of a highly diastereoselective but slower background reaction. Ligand to Cu ratio had no observable impact on reaction outcome in the range studied (0.9–1.2 equiv ligand to Cu).

It was found that reaction solvent had the largest impact on diastereoselectivity (*endo/exo*), enantioselectivity, and conversion as shown in Table 3.¹⁵ Etheral solvents tended to give

Table 3. Impact of Reaction Solvent on Stereoselectivity and Conversion^a

solvent	dr (<i>endo/exo</i>)	er <i>endo</i> product	conversion (%)
MTBE	9.1:1	90:10	34
CPME	8.1:1	98:2	>99
toluene	7.5:1	97:2	98
DME	5.5:1	92:8	63
2-MeTHF	5.3:1	99:1	98
THF	3.9:1	97:2	80

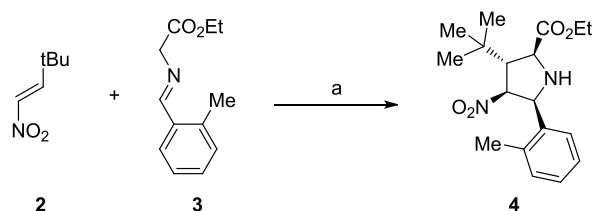
^aConditions: **2** (3.9 mmol, 1.0 equiv), **3** (4.3 mmol, 1.1 equiv), [Cu(OTf)₂·C₆H₆ (9.7 μmol, 0.25 mol %), **10** (21 μmol, 0.55 mol %), KOtBu (15 μmol, 0.40 mol %), 0 °C.

high conversion with the exception of MTBE, which was likely due to low catalyst solubility in this solvent as made evident by heterogeneity during precomplexation. While conversion and diastereoselectivity could be significantly improved on moving from the screening solvent tetrahydrofuran (THF) to 2-methyltetrahydrofuran (2-MeTHF), cyclopentyl methyl ether (CPME) was chosen as the reaction solvent due to the higher stereoselectivity and conversion observed in lab-scale experiments in this solvent and its low environmental impact.

Optimization studies culminated in the conditions chosen for scale-up of 0.25 mol % [Cu(OTf)₂·C₆H₆, 0.55 mol % **10**, and 0.4 mol % KOtBu in CPME (1 M in **2**) at 0 °C for 30 min giving an assay yield of 85%, dr of 8.1:1, and er of 98:2 (Scheme 5), but variability in the reaction outcome led us to investigate possible sources of irreproducibility before scale-up. Two contributing factors were identified: adventitious oxygen and purity of nitro olefin. To prevent catalyst decomposition from adventitious oxygen, plant runs employed an oxygen sensor to maintain O₂ levels below 10 ppm in reactors.¹⁶

Observed lot to lot variability in the nitro olefin led to a deeper investigation into impurities present in the starting material. As shown in Scheme 2, the final step in the synthesis of **2** is a TFAA mediated elimination to form the olefin. Consequently, nitro olefin lots had varying levels of the byproduct trifluoroacetic acid (TFA), which neutralizes the catalytic base charge in the [3 + 2] cycloaddition. TFA levels were determined by ion chromatography and ranged from 45

Scheme 5. Cu-Catalyzed Enantioselective [3 + 2] Cycloaddition^a



^aReagents and conditions: (a) **2** (1.0 equiv), **3** (1.1 equiv), [Cu(OTf)₂·C₆H₆ (0.25 mol %), **10** (0.55 mol %), KOtBu (0.40 mol %), CPME, −15 °C, 85% assay yield, 8.1:1 dr (*endo/exo*), 98.5:1.5 er.

to 16 000 ppm, which corresponded to 0.005–1.8 mol % with respect to limiting reagent **2**. These levels were sufficient to partially or fully neutralize the 0.4 mol % KOtBu charge, resulting in abrogation of reactivity. TFA levels in nitro olefin lots supplying plant campaigns were controlled to not more than 300 ppm because neutralization of acid by an increase of the base charge did not fully restore the reaction rate, although stereoselectivity was not impacted (Table 4). Reactions stalled

Table 4. Effect of Increasing KOtBu Charge in Cycloaddition of **2 Containing 1.39 mol % TFA**

KOtBu (mol %)	assay yield (%)	dr (<i>endo/exo</i>)	er <i>endo</i> product
1.79	51	8:1	98.8:1.2
2.79	45	8:1	98.7:1.3

at incomplete conversion without the presence of additional byproducts, suggesting premature catalyst decomposition. This result suggested that modification of the CuOTf/**10** complex by trifluoroacetate was occurring *in situ* to give a less stable or active catalytic species. Acceptable levels of TFA in **2** could be achieved by implementing additional sodium bicarbonate washes during workup.

Crystallization of Cycloaddition Product **2.** Because the reaction mixture contained catalytic Cu, **10**, and KOtBu, it was envisioned that a direct crystallization of **4** from the reaction mixture would be possible, obviating the need for a workup. To explore this, a solubility study was carried out on pure **4** (Figure 2). *n*-Heptane was found to be a suitable antisolvent

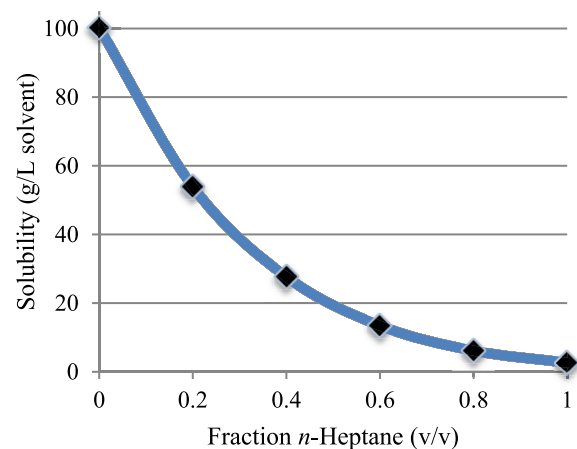


Figure 2. Solubility of **4** as a function of *n*-heptane fraction in CPME/*n*-heptane mixtures.

(solubility: 2.6 mg/mL) relative to the CPME reaction solvent (solubility: 101 mg/mL). At full conversion, the reaction reached a supersaturation ratio of approximately 2.9, resulting in spontaneous seed formation. The reaction mixture was subsequently concentrated by distillation and diluted with *n*-heptane to produce a readily filtered product slurry with acceptable product purity and loss to mother liquors.

The desired end-point for the crystallization was determined by exploring product purity and recovery as a function of solvent composition in lab-scale experiments. Major process-related impurities observed in the reaction crude were the imine **3** (present in 10% excess), diastereomer **11**, and enantiomer **12** (Figure 3).

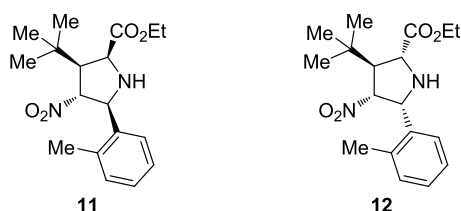


Figure 3. Reaction byproducts observed in [3 + 2] cycloaddition.

While a 5 L/kg process at 0.75 fraction *n*-heptane gave high-purity product (99.2 a%), product loss (9%) was deemed to be too high (Table 5). It was determined that lower (13% v/v) CPME fraction reduced the loss of product to the mother liquor to an acceptable level and did not significantly reduce product purity.

Table 5. Recovery and Purity of **4** by Crystallization from CPME/*n*-Heptane at 0 °C

fraction CPME	fraction heptane	total volume (L/kg 4)	loss of 4 to liquors (%)	11 in solid (a %)	purity of 4 (a%)
0.25	0.75	5.1	9	0.3	99.2
0.13	0.87	10.3	4	0.3	98.9

Further process intensification was achieved on scale-up by reducing the final volume from 10.3 to 3.5 L/kg with respect to **4** with no negative impact on isolated product purity.

Pilot Plant Campaign Results. The cycloaddition was executed in two pilot plant campaigns aimed at producing multikilogram quantities of ABBV-3221 for preclinical toxicology and clinical trial supply. Optimized reaction conditions were scaled to produce two 20 kg batches of product **4** in high enantiopurity and yield. Observations and modifications on scale are summarized in the following paragraphs.

On scale, control of the exotherm generated in the reaction was crucial to achieving high enantioselectivity. While lab runs on the gram scale gave a reaction er of 98.5:1.5 at 0 °C reactor temperature, the first campaign gave a reaction enantioselectivity of 96:4 er at 0 °C internal temperature. This result suggested that the rapid and exothermic cycloaddition reaction produced a feed zone of relatively higher temperature due to poorer mixing, which eroded the enantioselectivity. Control of the exotherm upon addition of nitro olefin by diluting the reactant in CPME to 1.6 L/kg, increasing the addition time from 0.5 to 3.5 h, and maintaining an internal temperature of not more than -10 °C was shown to improve enantioselectivity to 98.5:1.5 er in the second campaign.

Regardless of the reaction enantioselectivity, crystallization of the product from the reaction mixture took place readily on scale. After reaction completion, the mixture was concentrated to 0.5 L/kg **4**; *n*-heptane (3 L/kg **4**) was charged over 1 h, and then, the slurry was cooled to 0 °C over 4 h and filtered. The crystallization conditions resulted in rejection of the *exo* diastereomer **11** from a crude level of 8 a% to 0.3 a% and imine from 20 a% to 0.4 a% in the isolated product, while the enantiomer **12** level remained unchanged from the crude (1.5%). Crystallization studies of **4** at different enantiopurities suggested that there did not exist a significant difference in solubility between racemic and enantiopure crystal forms, resulting in an unavoidably poor rejection of enantiomer **12**. Nonetheless in the first pilot plant campaign, a very fine racemate solid was observed in the crystallization, which could be partially excluded by filtering the product into multiple portions to give a batch er of 97:3. Formation of the racemic solid, which had not been observed in lab-scale experiments, was attributed to lower reaction enantioselectivity (96:4 er) and uncontrolled nucleation during concentration of the reaction mixture rather than at reaction completion. In the second campaign, in which a reaction er of 98.5:1.5 was achieved, a total of 19.21 kg of **4** (78% yield) at 98.8a% purity (1.5% enantiomer) and 97.5% potency could be isolated directly from the reaction mixture through the crystallization process described above. The level of enantiomer **12** was acceptable because isolations downstream of this step resulted in rejection to <0.05a%.¹⁷

CONCLUSION

A highly enantioselective cycloaddition was developed to form the pyrrolidine core of ABBV-3221 from readily available starting materials. High-throughput screening validated an originally identified catalyst system, which was optimized by straightforward exploration of reaction parameters. Solvent choice was critical to improving selectivity and yield and also benefitted the isolation of cycloaddition product by enabling direct crystallization from the reaction mixture. Strict control of TFA in the nitro olefin starting material **2** was required to achieve reproducible reactivity, while a crude solution of imine **3** could be used directly after workup. The cycloaddition was carried out on a multikilogram scale to provide material for early deliveries of ABBV-3221 to supply preclinical and clinical trial demand.

EXPERIMENTAL DETAILS

General Remarks. Reagents and solvents were used as received without further purification. Reactions were carried out under nitrogen atmosphere. Large-scale reactions were carried out in pilot plant equipment (glass-lined reactors with agitator and jacket, stainless steel canisters) after a safety evaluation was completed. NMR spectra were obtained using a Varian 400 or 700 MHz NMR spectrometer. ¹H and ¹³C NMR chemical shifts are expressed in parts per million (δ) relative to CDCl₃ solvent. Analytical HPLC was performed on an Agilent 1100/1200 HPLC system equipped with either an Ascentis Express C18 (4.6 mm × 15 cm, 2.7 μm) or Chirapak IC (4.7 mm × 15 cm, 5 μm) column.

Preparation of Nitro Olefin (2). To the solution of pivalaldehyde (3.51 kg, 40.8 mol, 1 equiv) and MeNO₂ (2.74 kg, 44.8 mol, 1.1 equiv) in ethanol (7 L) was added NaOH (10 M, 5.3 L, 1.3 equiv) dropwise at 0 °C. The reaction

mixture was stirred at 0–10 °C for 0.5 h. HPLC showed that the reaction was complete. The reaction mixture was poured into water (14 L) and acidified with 6 M HCl until pH = 1–3 and extracted with MTBE (7 L × 3). The combined organic layers were washed with water (7 L) and brine (7 L), and dried over Na₂SO₄. The organic layers from three runs were concentrated to give **7** (16.5 kg, crude) as dark oil. Note: the crude product containing **7** and **2** was used directly in the next step without further purification.

Spectroscopic data for **7** matched previously measured values.¹⁰

To the crude solution of **7** and **2** (3.30 kg, 22.4 mol, 1.0 equiv) in CH₂Cl₂ (10.0 L) was added TFAA (5.42 kg, 25.8 mol, 3.59 L, 1.15 equiv) at –15 °C, and then, triethylamine (5.22 kg, 51.6 mol, 7.15 L, 2.30 equiv) was added dropwise, maintaining a reactor temperature below 10 °C. The mixture was stirred at –15 to 10 °C for 1 h. At reaction completion, the mixture was washed with saturated NH₄Cl aqueous solution (3 × 10 L), NaHCO₃ aqueous solution (5 L × 2), and brine (10 L), and dried over Na₂SO₄.

The organic layer was concentrated and purified by column chromatography on silica gel with petroleum ether to give **2** (9.35 kg, 72.4 mol, 64.6% yield, 99a% purity) as a yellow oil.

Spectroscopic data for **2** matched previously measured values.¹⁰

Preparation of Imine (3). To a suitable reactor was added glycine ethyl ester hydrochloride (15.3 kg, 110 mol, 1.1 equiv), sodium sulfate (28.4 kg, 200 mol, 2.0 equiv), methylene chloride (83 L, 1.20 M in *o*-tolualdehyde), and triethylamine (11.1 kg, 110 mol, 1.1 equiv). The thick slurry was stirred for 30 min at approximately 20 °C after which time *o*-tolualdehyde (12.0 kg, 100 mol, 1.0 equiv) was added. The reactor was stirred at approximately 20 °C for 2 h, at which point conversion reached >90% consumption of *o*-tolualdehyde as determined by ¹H NMR. The reaction mixture was then filtered and the filter washed with 34 L of methylene chloride. The product solution in methylene chloride was washed with water (2 × 60 L) and 23% sodium chloride solution (71 kg).

The organic layer was distilled to a volume of approximately 38 L. Then, a constant volume distillation with addition of CPME (55 L) was carried out until methylene chloride was present at less than 0.15 wt % to afford the product solution. The product solution was filtered through an in-line Teflon filter to a canister and the reactor rinsed with 4.7 L CPME to give **3** (18.98 kg, 98% purity, 45.2 wt %, 9.25 mol, 93% yield).

Data for **3** are as follows. ¹H NMR (700 MHz, CHCl₃): δ 8.60 (s, 1H), 7.92 (dd, *J* = 7.8, 1.5 Hz, 1H), 7.32 (td, *J* = 7.5, 1.5 Hz, 2H), 7.27–7.22 (m, 1H), 7.20–7.17 (m, 1H), 4.42 (d, *J* = 1.3 Hz, 2H), 4.24 (q, *J* = 7.1 Hz, 2H), 2.52 (s, 3H), 1.31 (t, *J* = 7.2 Hz, 3H). ¹³C NMR (176 MHz, CHCl₃): δ 170.3, 164.1, 138.0, 133.77, 130.9, 130.8, 127.9, 126.3, 62.7, 61.1, 19.4, 14.3.

Preparation of Pyrrolidine (4). Note: the reaction is sensitive to oxygen, and care must be taken to exclude oxygen until a passing reaction completion sample is obtained. To a reactor purged with N₂ to an O₂ level of approximately 10 ppm were added [Cu(OTf)₂] benzene complex (106 g, 0.18 mol, 0.25 mol %), ligand **10** (329 g, 0.40 mol, 0.55 mol %), and CPME (35 L) that had been previously sparged with N₂ for 1 h in a separate canister.

The resulting darkly colored suspension was stirred for 1 h at approximately 23 °C, after which time the reactor jacket was cooled to –25 °C. Imine **3** solution (36 kg, 45.2 wt %, 79 mol,

1.1 equiv), which had been previously sparged with N₂, was added at a rate such that the internal temperature did not exceed 0 °C. A 1.0 M potassium *tert*-butoxide solution in THF (260 g, 0.291 mol, 0.4 mol %) was added to the reactor and stirred for 15 min.

To a separate canister, nitro olefin **2** (9.33 kg, 72.2 mol, 1.0 equiv) and CPME (14.6 L) were charged and sparged by N₂. The nitrobutene solution was charged to the reactor at an O₂ level of less than ~10 ppm over 3 h 20 min (internal temp NMT –10 °C, targeted –15 °C). At reaction completion, the reactor was warmed to 23 °C.

The reaction mixture was distilled to a volume of approximately 30 L. After cooling to 23 °C, *n*-heptane (59 L) was added over 1 h. The reactor was stirred for 1 h at 23 °C after completed *n*-heptane addition and then cooled to 0 °C over 4 h. The slurry was then filtered and the filter cake washed with 19 L of *n*-heptane. The isolated material was dried at 50 °C to give **4** as a light brown crystalline solid (19.21 kg, 97.5% w/w, 56.0 mol, 77.6% yield, 98.8pa% purity, 1.5% enantiomer).

Data for **4** are as follows. ¹H NMR (700 MHz, CHCl₃): δ 7.27 (dd, *J* = 7.3, 1.8 Hz, 1H), 7.24–7.15 (m, 3H), 5.15 (dd, *J* = 6.1, 2.6 Hz, 1H), 4.53 (dd, *J* = 11.9, 6.1 Hz, 1H), 4.33 (qd, *J* = 7.1, 2.1 Hz, 2H), 3.79 (dd, *J* = 9.4, 7.3 Hz, 1H), 3.34–3.24 (m, 1H), 3.04 (dd, *J* = 7.3, 2.6 Hz, 1H), 2.39 (s, 3H), 1.35 (t, *J* = 7.2 Hz, 3H), 1.06 (s, 9H). ¹³C NMR (101 MHz, CHCl₃): δ 172.4, 135.1, 132.3, 130.4, 128.4, 126.4, 124.9, 91.6, 65.3, 61.8, 61.0, 32.6, 27.7, 19.5, 14.1. MS (APCI+): [M + H] calcd for C₁₈H₂₇N₂O₄, 335.4; found, 335.1.

Data for *exo* isomer **11** are as follows. ¹H NMR (400 MHz, CHCl₃): δ 7.77 (dd, *J* = 7.8, 1.4 Hz, 1H), 7.32–7.25 (m, 1H), 7.21 (td, *J* = 7.4, 1.5 Hz, 1H), 7.17–7.12 (m, 1H), 5.16 (t, *J* = 8.5 Hz, 1H), 4.95 (d, *J* = 8.4 Hz, 1H), 4.27 (m, 1H), 4.20 (m, 2H), 3.13 (t, *J* = 8.4 Hz, 1H), 2.29 (s, 3H), 2.19 (br s, 1H), 1.34 (t, *J* = 7.2 Hz, 2H), 1.02 (s, 9H). MS (APCI+): [M + H] calcd for C₁₈H₂₇N₂O₄, 335.4; found, 335.1.

■ ASSOCIATED CONTENT

📄 Supporting Information

The Supporting Information is available free of charge on the ACS Publications website at DOI: 10.1021/acs.oprd.9b00292.

Details of HTE catalyst screen, ¹H and ¹³C NMR of new compounds, HPLC trace analysis of cycloaddition products, and PXRD of **4** (PDF)

■ AUTHOR INFORMATION

Corresponding Author

*E-mail: john.hartung@abbvie.com.

ORCID

John Hartung: 0000-0001-5379-0307

Stephen N. Greszler: 0000-0003-1993-2417

Notes

The authors declare the following competing financial interest(s): All authors are employees of AbbVie. The design, study conduct, and financial support for this research were provided by AbbVie. AbbVie participated in the interpretation of data, review, and approval of the publication.

■ ACKNOWLEDGMENTS

The authors thank Robert W. Miller, Jerry G. Gaertner, Zhe Wang, and Brian Kotecki (all of AbbVie) for experimental assistance.

■ ABBREVIATIONS

MTBE, *tert*-butyl methyl ether; DME, dimethoxyethane

■ REFERENCES

- (1) Cutting, G. R. Cystic Fibrosis Genetics: From Molecular Understanding to Clinical Application. *Nat. Rev. Genet.* **2015**, *16*, 45–56.
- (2) Kerem, B.-S.; Rommens, J. M.; Buchanan, J. A.; Markiewicz, D.; Cox, T. K.; Chakravarti, A.; Buchwald, M.; Tsui, L.-C. Identification of the Cystic Fibrosis Gene: Genetic Analysis. *Science* **1989**, *245*, 1073–1080.
- (3) (a) Kartner, N.; Hanrahan, J. W.; Jensen, T. J.; Naismith, A. L.; Sun, S.; Ackerley, C. A.; Reyes, E. F.; Tsui, L.-C.; Rommens, J. M.; Bear, C. E.; Riordan, J. R. Expression of the Cystic Fibrosis Gene in Non-epithelial Invertebrate Cells Produces a Regulated Anion Conductance. *Cell* **1991**, *64*, 681–691. (b) Welsh, M. J.; Smith, A. E. Molecular Mechanisms of CFTR Chloride Channel Dysfunction in Cystic Fibrosis. *Cell* **1993**, *73*, 1251–1254.
- (4) Altenbach, R. J.; Bogdan, A.; Desroy, N.; Gfesser, G. A.; Greszler, S. N.; Koenig, J. R.; Kym, P. R.; Liu, B.; Scanio, M. J.; Searle, X.; Wang, X.; Yeung, M. C.; Zhao, G. Substituted Pyrrolidines as CFTR Modulators. *Intl. Pat. Appl.* 2018065962, 2018.
- (5) Wilson, R. M.; Danishefsky, S. J. Pattern Recognition in Retrosynthetic Analysis: Snapshots in Total Synthesis. *J. Org. Chem.* **2007**, *72*, 4293–4305.
- (6) For leading reviews, see: (a) Husinec, S.; Savic, V. Chiral Catalysts in the Stereoselective Synthesis of Pyrrolidine Derivatives via Metalloazomethine Ylides. *Tetrahedron: Asymmetry* **2005**, *16*, 2047–2061. (b) Pandey, G.; Banerjee, P.; Gadre, S. R. Construction of Enantiopure Pyrrolidine Ring System via Asymmetric [3 + 2]-Cycloaddition of Azomethine Ylides. *Chem. Rev.* **2006**, *106*, 4484–4517. (c) Stanley, L. M.; Sibi, M. P. Enantioselective Copper-Catalyzed 1,3-Dipolar Cycloadditions. *Chem. Rev.* **2008**, *108*, 2887–2902. (d) Hashimoto, T.; Maruoka, K. Recent Advances of Catalytic Asymmetric 1,3-Dipolar Cycloadditions. *Chem. Rev.* **2015**, *115*, 5366–5412.
- (7) For previous applications of enantioselective [3 + 2] cycloadditions on scale, see: (a) Shu, L.; Gu, C.; Fishlock, D.; Li, Z. Practical Synthesis of MDM2 Antagonist RG7388. Part 1: A Cu(II)-Catalyzed Asymmetric [3 + 2] Cycloaddition. *Org. Process Res. Dev.* **2016**, *20*, 2050–2056. (b) Rimmler, G.; Alker, A.; Bosco, M.; Diodone, R.; Fishlock, D.; Hildbrand, S.; Kuhn, B.; Moessner, C.; Peters, C.; Rege, P. D.; Schantz, M. Practical Synthesis of MDM2 Antagonist RG7388. Part 2: Development of the Cu(I) Catalyzed [3 + 2] Asymmetric Cycloaddition Process for the Manufacture of Idasanutin. *Org. Process Res. Dev.* **2016**, *20*, 2057–2066. (c) Shu, L.; Li, Z.; Gu, C.; Fishlock, D. Synthesis of a Spiroindolinone Pyrrolidinecarboxamide MDM2 Antagonist. *Org. Process Res. Dev.* **2013**, *17*, 247–256. (d) Agbodjan, A. A.; Cooley, B. E.; Copley, R. C. B.; Corfield, J. A.; Flanagan, R. C.; Glover, B. N.; Guidetti, R.; Haigh, D.; Howes, P. D.; Jackson, M. M.; Matsuoka, R. T.; Medhurst, K. J.; Millar, A.; Sharp, M. J.; Slater, M. J.; Toczko, J. F.; Xie, S. Asymmetric Synthesis of an N-Acylpyrrolidine for Inhibition of HCV Polymerase. *J. Org. Chem.* **2008**, *73*, 3094–3102.
- (8) (a) Yan, X.-X.; Peng, Q.; Zhang, Y.; Zhang, K.; Hong, W.; Hou, X.-L.; Wu, Y.-D. A Highly Enantio- and Diastereoselective Cu-Catalyzed 1,3-Dipolar Cycloaddition of Azomethine Ylides with Nitroalkenes. *Angew. Chem., Int. Ed.* **2006**, *45*, 1979–1983. (b) Arai, T.; Mishiro, A.; Yokoyama, N.; Suzuki, K.; Sato, H. Chiral Bis(imidazolidine)pyridine-Cu(OTf)₂: Catalytic Asymmetric Endo-Selective [3 + 2] Cycloaddition of Imino Esters with Nitroalkenes. *J. Am. Chem. Soc.* **2010**, *132*, 5338–5339. (c) Li, J.-Y.; Kim, H. Y.; Oh, K. Brucine Diol-Copper-Catalyzed Asymmetric Synthesis of *endo*-Pyrrolidines: The Mechanistic Dichotomy of Imino Esters. *Org. Lett.* **2015**, *17*, 1288–1291. (d) Conde, E.; Rivilla, I.; Larumbe, A.; Cossio, F. P. Enantiodivergent Synthesis of Bis-Spiropyrrolidines via Sequential Interrupted and Completed (3 + 2) Cycloadditions. *J. Org. Chem.* **2015**, *80*, 11755–11767.
- (9) Ballini, R.; Petrini, B. The Nitro to Carbonyl Conversion (Nef Reaction): New Perspectives for a Classical Transformation. *Adv. Synth. Catal.* **2015**, *357*, 2371–2402.
- (10) Denmark, S. E.; Marcin, L. R. Asymmetric Nitroalkene [4 + 2] Cycloadditions: Enantioselective Synthesis of 3-Substituted and 3,4-Disubstituted Pyrrolidines. *J. Org. Chem.* **1995**, *60*, 3221–3235.
- (11) CPME was investigated as the reaction solvent because it would enable more efficient workup and telescoping. However, this met with no success because conversion to the desired product was not observed.
- (12) Onset of an exothermic event was observed at 62 °C when heating isolated **3** during a routine safety evaluation.
- (13) The development and application of this methodology will be disclosed in a future publication.
- (14) Strong base was used because it has been shown to suppress formation of the Michael adduct from the stepwise reaction of the azomethine ylides with nitro olefins. See ref 8a for details.
- (15) The solvent effect was also observed in the initial disclosure of the catalyst system (ref 8a). The higher dr observed in less polar solvents is consistent with the authors' proposal that the *endo* transition state is stabilized by an electrostatic interaction.
- (16) A 13% drop in yield was observed in reactions run under an atmosphere of air.
- (17) Analysis for Cu content was carried out downstream of this step and was found to be at an acceptable level per ICH Q3D.